Seminar Recent Advances in Geometry Processing

SuGaR: Surface-Aligned Gaussian Splatting for Efficient 3D Mesh Reconstruction and High-Quality Mesh Rendering

Bertan Karacora
University of Bonn
bertan.karacora@uni-bonn.de

Abstract

Reconstructing the surface geometry and the visual appearance of 3D scenes is fundamental for creating high-quality, editable scene representations. 3D Gaussian Splatting (3DGS) has recently gained a lot of attention as a scene modeling approach, enabling real-time photorealistic rendering and fast training. However, the unstructured and volumetric nature of the 3D Gaussians poses challenges for geometry reconstruction. This report deals with SuGaR [5], a method proposed by Guédon and Lepetit that allows for accurate and efficient mesh extraction from 3DGS. SuGaR modifies the optimization process of 3DGS using a regularization term to align the Gaussians with the surface. Subsequently, it employs Poisson reconstruction to create a mesh representation of the surface which can be extended and refined by binding Gaussians to the mesh. In their work, Guédon and Lepetit demonstrate SuGaR's ability for surface reconstruction, showcasing applications such as scene composition and animation, while maintaining real-time, high-fidelity rendering. Although the surface-alignment approach increases geometric consistency, SuGaR tends to miss fine details, and restricts the model's capacity to capture the visual appearance.

1. Introduction

Accurately reconstructing 3D scenes given a set of multi-view images is a crucial problem in computer vision and graphics, with applications including virtual and augmented reality [21], avatar creation [16], and robotics [17]. In particular, capturing a scene's surface geometry as a polygonal mesh allows for editing, physics simulations, and compatibility with common 3D graphics tools. In contrast, more flexible scene representations such as radiance fields have shown superior potential for novel view synthesis, the task of generating realistic images from arbitrary viewpoints. As a key challenge, it is critical to balance visual expressiveness and geometric constraint to account for both photorealistic rendering and geometric control.

Recently, 3D Gaussian Splatting (3DGS) [9] has achieved impressive results for real-time novel view synthesis. Its core idea is to approximate the process of differentiable volume rendering using rasterization of explicit volumetric primitives rather than ray-sampling over a continuous radiance field, resulting in much faster rendering and training. More precisely, 3DGS represents a scene as a set of 3D Gaussians, each parametrized by their position, orientation, scales, opacity, and view-dependent color. For rendering, the Gaussian contribute as splats in the viewing plane, composited using alpha blending. Despite its ability to capture a scene's appearance, the optimized Gaussians typically do not align well with the surface, and the sparse approximation of the radiance field makes it difficult to extract a consistent surface representation.

SuGaR [5], as proposed by Guédon and Lepetit, constitutes a method to extend 3DGS to capture both appearance and geometry. To this end, it regularizes the 3DGS optimization, enforcing alignment of the volume density approximated by the Gaussians with a target density derived under the assumption that the Gaussians are flat and well distributed over the surface. It then samples oriented points on the level set of the estimated density and extracts a globally consistent and smooth surface via Poisson reconstruction [8], mitigating artifacts from the sparse density distribution. Finally, a Gaussian-mesh hybrid representation can be created by binding Gaussians to the mesh, enabling high-quality 3DGS rendering of the mesh, indirect control over the Gaussians using the underlying mesh, and further optimization of the mesh geometry using 3DGS optimization.

This report aims to give a condensed description of the work of Guédon and Lepetit [5] while adding own explanations and critical thought. Therefore, the following elaborates on the essential ideas, methods, and experimental results. Additionally, it discussed some more recent developments in 3DGS-based surface reconstruction.

Figure 1. SuGaR allows to efficiently extract meshes that can be used for applications like editing, scene composition, and animation. The top row shows input images of different scenes, composited in the bottom image.

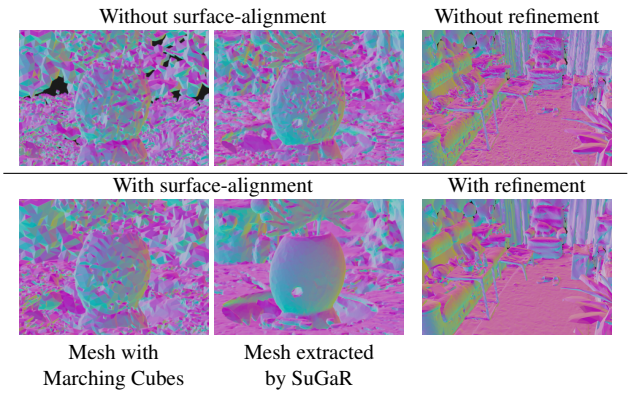

Figure 2. Effect of regularization, mesh extraction method, and refinement. Only the combination of surface-aligment and SuGaR's mesh extraction leads to a smooth and consistent mesh. The refinement step further improves its quality.

2. Related work

Photogrammetry Traditional structure-from-motion (SfM) methods like COLMAP [15] handle the image-based scene reconstruction problem as a series of subproblems including pairwise camera calibration, and triangulation, resulting in camera poses and a sparse 3D point cloud. Given these, multi-view stereo (MVS) (e.g., patch-based MVS[4]) infers dense depth maps using image matching and triangulation.

These methods rely heavily on explicit geometry constraints and handcrafted heuristics, making them struggle with textureless, or transparent surfaces, as well as occlusions. They involve a long pipeline of complex optimization steps, leading to high computational requirements and noisy results. Moreover, generating photorealistic novel views from point clouds or depth maps remains challenging. These limitations have led to the rise of learning-based methods, which focus on volumetric representations for a differentiable, and more robust scene reconstruction.

Neural radiance fields Neural radiance fields (NeRFs) [13] have recently become a powerful approach for novel view synthesis and 3D geometry reconstruction. As a volumetric representation, NeRF allows to model fuzzy, shiny, and translucent materials more directly than surface-based scene models. Furthermore, its representation allows for differentiable volume rendering, massively simplifying the optimization procedure.

Originally designed for novel view synthesis, NeRFs have been extended to also enable surface reconstruction. Instead of directly learning the radiance field, models like NeuS [19] and Neuralangelo [11] learn a signed distance function, representing the surface, and transform it to arrive at the radiance field. NeRFs achieve accurate reconstruction and realistic rendering, however, they suffer from slow rendering speed and excessive training times. Adressing these issues, 3D Gaussian Splatting (3DGS) [9] approximates the implicit radiance field representation using explicit scene primitives, and replaces the costly ray-marching-based volume rendering with efficient rasterization.

3. Methods

Given a set of images with corresponding camera poses and intrinsics, SuGaR's goal is to efficiently reconstruct a 3D scene's surface as a mesh while allowing for high-quality real-time rendering. To achieve this, it adopts the scene model of 3DGS [9], modifies its optimization process to incorporate a surface-alignment regularization, and efficiently extracts a mesh using Poisson Reconstruction [8]. By binding new Gaussians to it, the mesh can be further refined and rendered naturally using 3DGS. Figure 2 visualizes the effect of each step.

3.1. Preliminary

Radiance Fields and Volume Rendering 3DGS uses the same differentiable volume rendering formulation as NeRF [13]. In NeRF, the appearance of a scene is modeled implicitly as a continuous radiance field that maps each 3D point $\mathbf{x}$ to a volume density $\sigma_{\mathbf{x}}$ and a viewing direction-conditioned color $\mathbf{c}_{\mathbf{x}}$. A pixel's color $\mathbf{c}$ is then calculated by alpha blending samples of the radiance field along the viewing ray at intervals θ_i:

$$\mathbf{c} = \sum_{i=1}^{N} \mathbf{c}_i \alpha_i \prod_{j=1}^{i-1} (1-\alpha_i), \text{ with } \alpha_i = 1 - \exp\left(-\sigma_i \theta_i\right). \quad (1)$$

3D Gaussian Splatting (3DGS) 3DGS [9] explicitly represents a scene as a set of 3D Gaussian primitives $\{g_k\}$,

where each Gaussian is defined by a position $\mathbf{p}_k$, scaling factors $\mathbf{s}_k$, quaternion $\mathbf{q}_k$, opacity α_k, and color $\mathbf{c}_k$ encoded in real spherical harmonics. The alpha blending coefficients are now approximated using opacities $\{\alpha_k\}$ and Gaussians

$$\mathcal{G}_k(\mathbf{x}) = \exp\left(-\frac{1}{2}(\mathbf{x}-\mathbf{p}_k)^\intercal \mathbf{\Sigma}_k^{-1}(\mathbf{x}-\mathbf{p}_k)\right), \quad (2)$$

where $\mathbf{\Sigma}_k = \mathbf{RSS}^\intercal\mathbf{R}^\intercal$ is the 3D covariance matrix composed from the quaternion-encoded rotation $\mathbf{R}$ and diagonal scaling matrix $\mathbf{S}$. For efficient rasterization-style rendering, each Gaussian's contribution in 2D is efficiently precomputed and splatted onto the image plane [25]. The scene model is trained via self-supervision using a photometric loss and gradient-based optimization.

3.2. Surface-alignment regularization

The 3DGS scene representation is volumetric and unstructured in nature, causing challenges for surface reconstruction. Additionally, 3DGS has great representation power due to the anisotropy of the Gaussians and the view-dependent color, which is advantageous for novel view synthesis but leads to misaligned Gaussians that do not correspond well to the true surface. To increase geometric consistency and facilitate mesh extraction, SuGaR regularizes the Gaussians to approximate a volume density assuming an ideal case, where the Gaussians are flat, opaque and evenly distributed over the surface.

Specifically, SuGaR considers the local density measure

$$d(\mathbf{p}) = \sum_k \alpha_k \mathcal{G}_k(\mathbf{p}). \quad (3)$$

Assuming the Gaussians are opaque and have limited overlap, the density is dominated by the closest Gaussian g_{k^*} and we can approximate it as

$$d(\mathbf{p}) \approx \exp\left(-\frac{1}{2}(\mathbf{x}-\mathbf{p}_{k^*})^\intercal \Sigma_{k^*}^{-1}(\mathbf{x}-\mathbf{p}_{k^*})\right). \quad (4)$$

Further, we can decompose the covariance and consider the magnitude of the eigenvalues, assuming a flat Gaussian:

$$\Sigma_k = V\text{diag}(s_1^2, s_2^2, s_3^2)V^\intercal, \text{ with } s_{k^*} = s_3 \ll s_1, s_2. \quad (5)$$

Now, the density further simplifies to

$$(\mathbf{x}-\mathbf{p}_{k^*})^\intercal \Sigma_{k^*}^{-1}(\mathbf{x}-\mathbf{p}_{k^*}) = \sum_{i=1}^{3} \frac{1}{s_i^2}\langle \mathbf{x}-\mathbf{p}_{k^*}, \mathbf{v}_i\rangle^2, \quad (6)$$

$$\bar{d}(\mathbf{p}) \approx \frac{1}{s_{k^*}^2}\langle \mathbf{x}-\mathbf{p}_{k^*}, \mathbf{n}_{k^*}\rangle^2, \quad (7)$$

where we define $\bar{d}$ as the approximated density in the ideal scenario and $\mathbf{n}_{k^*}$ as the normal of the flat Gaussian.

In practice, SuGaR proposes multiple regularization strategies, one of which is to minimize $\left|\bar{d}(\mathbf{p}) - d(\mathbf{p})\right|$. However, for better handling the sparse density and a more global supervision that considers multiple Gaussians simultaneously, SuGaR recommends to further transform the density to the signed distance function (SDF) $f(\mathbf{p}) = \pm s_{k^*}\sqrt{-2\log\left(d(\mathbf{p})\right)}$. For supervision, it samples values $\hat{f}(\mathbf{p})$ as the offset of visible point $\mathbf{p}$ from the depth map that can be easily rendered using 3DGS. Finally, we arrive at the regularization term that is added to the 3DGS optimization:

$$R_{\text{align}} = \frac{1}{|\mathcal{P}|}\sum_{\mathbf{p}\in\mathcal{P}}\left|\hat{f}(\mathbf{p}) - f(\mathbf{p})\right|, \quad (8)$$

where $\mathcal{P}$ is a set of points sampled from the scene.

3.3. Mesh extraction

Once the Gaussians are aligned with the scene surface, SuGaR extracts a mesh by identifying a level set of the density function d. In constrast to Marching Cubes [12], which requires dense sampling of the 3D volume, SuGaR efficiently determines surface points through ray-guided sampling. First, SuGaR unprojects the rendered depth maps to generate 3D point clouds. For each 3D point, it performs a local search along its viewing ray, guided by the standard deviation of the nearest Gaussian in ray direction. SuGaR samples the density function at a fixed number of points along the ray and linearly interpolates the first point that reaches the desired iso-value. This approach is particularly efficient, as it scales linearly with the number of pixels.

Using only these samples of the level set, SuGaR applies Poisson reconstruction [8]. This method estimates an indicator function whose gradient aligns with surface and its normals, allowing for smooth, globally consistent mesh extraction. The local normal is computed as the gradient of the density $\frac{\nabla d(\hat{p})}{\|\nabla d(\hat{p})\|_2}$. Notably, unlike Marching Cubes [12], Poisson reconstruction does not suffer from heavy artifacts resulting from the sparsity of the volume density.

3.4. Hybrid representation and refinement

After extracting the mesh, SuGaR enables a hybrid representation by binding new Gaussians to the mesh. These Gaussians are parametrized relative to the underlying mesh, i.e., their positions are computed using the mesh vertices and predefined barycentric coordinates, and their orientation is fixed to align with the triangle's plane. Consequently, the 3DGS optimization can now backpropagate gradients to the positions of the mesh vertices, and a learnable 2D rotation within the local surface plane. This integration allows for native refinement of the mesh as well as high-quality rendering of the mesh using the 3DGS renderer. Additionally, since the Gaussians are directly bound to the mesh structure, standard mesh editing tools can be used to manipulate the 3DGS scene.

4. Experiments and results

Guédon and Lepetit [5] evaluate their work quantitatively only for the task of novel view synthesis in real-world 3D scenes. For a better comparison, this report also takes more recent methods into account, including results from 2DGS [6], evaluating SuGaR's surface reconstruction capabilities. Due to the space constraints of this report, no details on the implementation, no ablations and no additional qualitative results are included.

4.1. Surface Reconstruction

Table 1 shows a comparison of SuGaR's refined meshes with the state-of-the-art in surface reconstruction. Whereas the DTU dataset [7] is provided with rather accurate ground truth for the evaluation using the Chamfer distance, Tanks and Temples dataset (TnT) [10] includes more large-scale scenes, significantly more images, and is evaluated using the F1 metric that does not consider small deviations.

SuGaR does considerably improve the surface quality compared to the original 3DGS, however, most recent NeRF-based works and more recent ones using 3DGS outperform SuGaR. All surface reconstruction methods based on explicit representations are much faster than the implicit-based ones, but SuGaR is slower than more recent works.

		DTU		TnT	
		CD ↓	Time ↓	F1 ↑	Time ↓
implicit	NeRF [13]	1.49	> 12h	-	-
	NeuS [19]	0.84	> 12h	0.38	> 24h
	Neuralangelo [11]	0.61	> 12h	0.50	> 128h
explicit	3DGS [9]	1.96	0.2h	0.09	0.2h
	SuGaR [5]	**1.33**	**1h**	**0.19**	**2h**
	2DGS [6]	0.80	0.3h	0.32	0.6h
	GOF [23]	0.74	2h	0.46	2h
	PGSR [2]	0.53	0.6h	0.52	0.8h
	GausSurf [18]	0.52	0.1h	0.50	0.6h

Table 1. Quantitative comparison on the DTU and TnT datasets. The Chamfer distance (CD), F1 score, and optimization times averaged over all scenes for each dataset are shown. , , indicate the best, the second best, and the third best result respectively. Results are taken from the respective papers, if available.

4.2. Novel View Synthesis

The rendering quality of SuGaR's Gaussian-mesh hybrid is compared to state-of-the-art NeRF-based approaches as well as ones using 3DGS for surface reconstruction. Table 2 shows the results on the Mip-NeRF 360 dataset [1] using the standard metrics PSNR, SSIM and LPIPS [24].

Notably, SuGaR achieves competitive results compared to NeRF-based methods that do not explicitly reconstruct a surface mesh, while also allowing for real-time rendering. However, the restricting the Gaussians to the surface limits the model's ability to capture the visual appearance, as can be seen from the decreased performance compared to vanilla 3DGS.

	Outdoor scenes			Indoor scenes		
	PSNR ↑	SSIM ↑	LPIPS ↓	PSNR ↑	SSIM ↑	LPIPS ↓
NeRF [13]	21.46	0.458	0.515	26.84	0.790	0.370
Instant NGP [14]	22.90	0.566	0.371	29.15	0.880	0.216
MipNeRF360 [1]	24.47	0.691	0.283	31.72	0.917	0.180
3DGS [9]	24.64	0.731	0.234	30.41	0.920	0.189
SuGaR [5]	**22.93**	**0.629**	**0.356**	**29.43**	**0.906**	**0.225**
2DGS [6]	24.34	0.717	0.246	30.40	0.916	0.195
GOF [23]	24.76	0.742	0.225	30.80	0.928	0.167
PGSR [2]	24.45	0.730	0.224	30.41	0.930	0.161
GausSurf [18]	25.09	0.753	0.212	30.05	0.920	0.183

Table 2. Quantitative results on the Mip-NeRF 360 dataset. All results are taken from the respective papers, if available.

5. Discussion

SuGaR [5] is one of the first methods that leverage 3DGS for surface reconstruction. Therefore, SuGaR introduces a novel approach that combines real-time photorealistic rendering and geometric control, a valuable possibility for scene reconstruction with many practical applications.

Many recent works have followed the concepts of SuGaR. 2D Gaussian Splatting (2DGS) [6] extends SuGaR's idea by callapsing the Gaussians completely to 2D, improving multi-view geometric consistency and mesh reconstruction. The state-of-the-art method PGSR [2] compresses 3D Gaussians into flat planes to render unbiased depth and normal maps for geometry reconstruction. NeuSG [3] jointly optimizes Neuralangelo [11] and 3DGS, using SDF-based normals to refine Gaussian orientations.

Despite these advances, SuGaR has notable limitations. The proposed regularization term restricts the model's flexibility, leading to lower rendering quality than standard 3DGS. Moreover, SuGaR's 3D reconstructions tend to miss details, and are susceptible to artifacts, resulting from the assumption that a single Gaussian dominates the local density [20]. Additionally, recent works have pointed out that the depth-based supervision of the regularization is inaccurate and biased [2].

While SuGaR bridges the gap between 3DGS-based rendering and surface extraction, future work could focus on solving the conflict of flexibile appearance and geometric constraint. As an example, GSDF [22] combines 3DGS and a SDF surface representation, demonstrating mutual guidance during optimization.

6. Conclusion

SuGaR extends 3D Gaussian Splatting by introducing surface alignment and Poisson reconstruction to extract accurate meshes while preserving real-time rendering. This approach improves geometric consistency and enables scene editing, but comes at the cost of reduced flexibility in capturing fine visual details. Despite these trade-offs, SuGaR represents a notable step toward integrating the strengths of different representations into a single scene model.

References

[1] Ben Barron, Jonathan T. and Mildenhall, Dor Verbin, and Peter Srinivasan, Pratul P. and Hedman. Mip-NeRF 360: Unbounded Anti-Aliased Neural Radiance Fields. In *Proceedings of the IEEE/CVF conference on computer vision and pattern recognition*, pages 5470–5479, 2022. 4

[2] Danpeng Chen, Hai Li, Weicai Ye, Yifan Wang, Weijian Xie, Shangjin Zhai, Nan Wang, Haomin Liu, Hujun Bao, and Guofeng Zhang. PGSR: Planar-based Gaussian Splatting for Efficient and High-Fidelity Surface Reconstruction. *IEEE Transactions on Visualization and Computer Graphics*, 2024. 4

[3] Hanlin Chen, Chen Li, and Gim Hee Lee. Neusg: Neural implicit surface reconstruction with 3d gaussian splatting guidance. *arXiv preprint arXiv:2312.00846*, 2023. 4

[4] Yasutaka Furukawa and Jean Ponce. Accurate, dense, and robust multiview stereopsis. *IEEE transactions on pattern analysis and machine intelligence*, 32(8):1362–1376, 2009. 2

[5] Antoine Guédon and Vincent Lepetit. SuGaR: Surface-Aligned Gaussian Splatting for Efficient 3D Mesh Reconstruction and High-Quality Mesh Rendering. In *Proceedings of the IEEE/CVF Conference on Computer Vision and Pattern Recognition*, pages 5354–5363, 2024. 1, 4

[6] Binbin Huang, Zehao Yu, Anpei Chen, Andreas Geiger, and Shenghua Gao. 2D Gaussian Splatting for Geometrically Accurate Radiance Fields. In *SIGGRAPH 2024 Conference Papers*. Association for Computing Machinery, 2024. 4

[7] Rasmus Jensen, Anders Dahl, George Vogiatzis, Engin Tola, and Henrik Aanæs. Large Scale Multi-view Stereopsis Evaluation. In *Proceedings of the IEEE conference on computer vision and pattern recognition*, pages 406–413, 2014. 4

[8] Michael Kazhdan, Matthew Bolitho, and Hugues Hoppe. Poisson Surface Reconstruction. In *Proceedings of the fourth Eurographics symposium on Geometry processing*, 2006. 1, 2, 3

[9] Bernhard Kerbl, Georgios Kopanas, Thomas Leimkühler, and George Drettakis. 3D Gaussian Splatting for Real-time Radiance Field Rendering. *ACM Trans. Graph.*, 42(4):139–1, 2023. 1, 2, 4

[10] Arno Knapitsch, Jaesik Park, Qian-Yi Zhou, and Vladlen Koltun. Tanks and Temples: Benchmarking Large-Scale Scene Reconstruction. *ACM Transactions on Graphics (ToG)*, 36(4):1–13, 2017. 4

[11] Zhaoshuo Li, Thomas Müller, Alex Evans, Mathias Taylor, Russell H. and Unberath, Ming-Yu Liu, and Chen-Hsuan Lin. Neuralangelo: High-Fidelity Neural Surface Reconstruction. In *Proceedings of the IEEE/CVF Conference on Computer Vision and Pattern Recognition*, pages 8456–8465, 2023. 2, 4

[12] Harvey E. Lorensen, William E. and Cline. Marching cubes: A high resolution 3D surface construction algorithm. In *Seminal graphics: pioneering efforts that shaped the field*, pages 347–353. 1998. 3

[13] Ben Mildenhall, Pratul P Srinivasan, Matthew Tancik, Jonathan T Barron, Ravi Ramamoorthi, and Ren Ng. NeRF: Representing Scenes as Neural Radiance Fields for View Synthesis. In *European Conference on Computer Vision*, 2020. 2, 4

[14] Thomas Müller, Alex Evans, Christoph Schied, and Alexander Keller. Instant Neural Graphics Primitives with a Multiresolution Hash Encoding. *ACM Trans. Graph.*, 41(4):1–15, 2022. 4

[15] Johannes L Schonberger and Jan-Michael Frahm. Structure-from-Motion Revisited. In *Proceedings of the IEEE conference on computer vision and pattern recognition*, pages 4104–4113, 2016. 2

[16] Zhijing Shao, Zhaolong Wang, Zhuang Li, Duotun Wang, Xiangru Lin, Yu Zhang, Mingming Fan, and Zeyu Wang. SplattingAvatar: Realistic Real-Time Human Avatars with Mesh-Embedded Gaussian Splatting. In *Proceedings of the IEEE/CVF Conference on Computer Vision and Pattern Recognition*, pages 1606–1616, 2024. 1

[17] Fabio Tosi, Youmin Zhang, Ziren Gong, Erik Sandström, Stefano Mattoccia, Martin R Oswald, and Matteo Poggi. How NeRFs and 3D Gaussian Splatting are Reshaping SLAM: a Survey. *arXiv preprint arXiv:2402.13255*, 4, 2024. 1

[18] Jiepeng Wang, Yuan Liu, Peng Wang, Cheng Lin, Junhui Hou, Xin Li, Taku Komura, and Wenping Wang. GausSurf: Geometry-Guided 3D Gaussian Splatting for Surface Reconstruction. *arXiv preprint arXiv:2411.19454*, 2024. 4

[19] Peng Wang, Lingjie Liu, Yuan Liu, Christian Theobalt, Taku Komura, and Wenping Wang. NeuS: Learning Neural Implicit Surfaces by Volume Rendering for Multi-view Reconstruction. *Advances in Neural Information Processing Systems*, 2021. 2, 4

[20] Qianyi Wu, Jianmin Zheng, and Jianfei Cai. Surface reconstruction from 3d gaussian splatting via local structural hints. In *European Conference on Computer Vision*, pages 441–458. Springer, 2024. 4

[21] Linning Xu, Vasu Agrawal, William Laney, Tony Garcia, Aayush Bansal, Changil Kim, Samuel Rota Bulò, Lorenzo Porzi, Peter Kontschieder, Aljaž Božič, et al. VR-NeRF: High-Fidelity Virtualized Walkable Spaces. In *SIGGRAPH Asia 2023 Conference Papers*, pages 1–12, 2023. 1

[22] Mulin Yu, Tao Lu, Linning Xu, Lihan Jiang, Yuanbo Xiangli, and Bo Dai. GSDF: 3DGS Meets SDF for Improved Neural Rendering and Reconstruction. *Advances in Neural Information Processing Systems*, 37:129507–129530, 2024. 4

[23] Zehao Yu, Torsten Sattler, and Andreas Geiger. Gaussian Opacity Fields: Efficient Adaptive Surface Reconstruction in Unbounded Scenes. *ACM Transactions on Graphics*, 2024. 4

[24] Richard Zhang, Phillip Isola, Alexei A Efros, Eli Shechtman, and Oliver Wang. The Unreasonable Effectiveness of Deep Features as a Perceptual Metric. In *Proceedings of the IEEE conference on computer vision and pattern recognition*, pages 586–595, 2018. 4

[25] Matthias Zwicker, Hanspeter Pfister, Jeroen Van Baar, and Markus Gross. EWA Volume Splatting. In *Proceedings Visualization, 2001. VIS'01.*, pages 29–538. IEEE, 2001. 3